Radial electric field and transport near the rational surface and the magnetic island in LHD



2004 Nucl. Fusion 44 290

(http://iopscience.iop.org/0029-5515/44/2/010)

INSTITUTE OF PHYSICS PUBLISHING and INTERNATIONAL ATOMIC ENERGY AGENCY NUCLEAR FUSION

Nucl. Fusion **44** (2004) 290–295 PII: S0029-5515(04)73464-X

# Radial electric field and transport near the rational surface and the magnetic island in LHD

**K. Ida[1], S. Inagaki[1], N. Tamura[1], T. Morisaki[1], N. Ohyabu[1], K. Khlopenkov[1], S. Sudo[1], K. Watanabe[1], M. Yokoyama[1], T. Shimozuma[1], Y. Takeiri[1], K. Itoh[1], M. Yoshinuma[1], Y. Liang[1], K. Narihara[1], K. Tanaka[1], Y. Nagayama[1], T. Tokuzawa[1], K. Kawahata[1], H. Suzuki[1], A. Komori[1], T. Akiyama[1], N. Ashikawa[1], M. Emoto[1], H. Funaba[1], P. Goncharov[2], M. Goto[1], H. Idei[1], K. Ikeda[1], M. Isobe[1], O. Kaneko[1], H. Kawazome[3], T. Kobuchi[1], A. Kostrioukov[2], S. Kubo[1], R. Kumazawa[1], S. Masuzaki[1], T. Minami[1], J. Miyazawa[1], S. Morita[1], S. Murakami[1], S. Muto[1], T. Mutoh[1], Y. Nakamura[1], H. Nakanishi[1], Y. Narushima[1], K. Nishimura[1], N. Noda[1], T. Notake[4], H. Nozato[5], S. Ohdachi[1], Y. Oka[1], M. Osakabe[1], T. Ozaki[1], B.J. Peterson[1], A. Sagara[1], T. Saida[6], K. Saito[1], S. Sakakibara[1], R. Sakamoto[1], M. Sasao[6], K. Sato[1], M. Sato[1], T. Seki[1], M. Shoji[1], N. Takeuchi[4], K. Toi[1], Y. Torii[4], K. Tsumori[1], T. Watari[1], Y. Xu[1], H. Yamada[1], I. Yamada[1], S. Yamamoto[4], T. Yamamoto[4], Y. Yoshimura[1], I. Ohtake[1], K. Ohkubo[1], T. Mito[1], T. Satow[1], T. Uda[1], K. Yamazaki[1], K. Matsuoka[1], O. Motojima[1] and M. Fujiwara[1]**

[1] National Institute for Fusion Sciences, Toki, Gifu 509-5292, Japan
[2] Department of Fusion Science, School of Mathematical and Physical Science, Graduate University for Advanced Studies, Hayama 240-0193, Japan
[3] Graduate School of Energy Science, Kyoto University, Uji 611-0011, Japan
[4] Department of Energy Engineering and Science, Nagoya University, 464-8603, Japan
[5] Graduate School of Frontier Sciences, The University of Tokyo, 113-0033, Japan
[6] Tohoku University, Japan

Received 12 December 2002, accepted for publication 16 December 2003
Published 12 January 2004
Online at stacks.iop.org/NF/44/290 (DOI: 10.1088/0029-5515/44/2/010)

**Abstract**
The structure of the radial electric field and heat transport at the magnetic island in the large helical device (LHD) are investigated by measuring the radial profile of the poloidal flow with charge exchange spectroscopy and measuring the time evolution of the electron temperature with ECE. A vortex-like plasma flow along the magnetic flux surface inside the magnetic island is observed when the $n/m = 1/1$ external perturbation field becomes large enough to increase the magnetic island width above a critical range (15–20% of minor radius) in LHD. This convective poloidal flow results in a non-flat space potential inside the magnetic island. The sign of the curvature of the space potential ($\partial^2\Phi/\partial r^2$, where $\Phi$ is the space potential) depends on the radial electric field at the boundary of the magnetic island. The heat transport inside the magnetic island is studied with a cold pulse propagation technique. The experimental results show the existence of radial electric field shear at the boundary of the magnetic island and a reduction in heat transport at the boundary and inside the magnetic island.

**PACS numbers:** 52.55.Hc, 52.50.Gj

## 1. Introduction

The structure of the magnetic island is observed under various plasma parameters. The electron temperature profiles measured with Thomson scattering or ECE signals show flattening inside the magnetic island [1–3]. If the space potential is not flat inside the magnetic island, both the radial electric field and the poloidal flow should be finite inside the magnetic island. Because of the conservation of particle flux along the magnetic flux surface, the plasma flow should be vortex-like inside the magnetic island, if it exists. When there is vortex-like plasma inside the magnetic island, the

  

sign of the radial electric field should be reversed across the centre of the magnetic island, and radial electric field shear should appear inside the magnetic island. Therefore, there are two states in plasma flow and space potential predicted. In one, there is no plasma flow inside the magnetic island and hence no radial electric field and flat space potential. In the other, there is a vortex-like plasma flow, finite radial electric field and non-flat space potential inside the magnetic island. Although it is unknown which state is realized in the plasma, there have been few clear measurements of plasma flow or radial electric field inside the magnetic island [4,5]. The large helical device (LHD) [6] is a Heliotron device (poloidal period number $L = 2$ and toroidal period number $M = 10$) with a major radius of $R_{ax} = 3.5$–$4.1$ m, an average minor radius of 0.6 m and magnetic field up to 3 T. The radial electric field ($E_r$) is derived from the poloidal and toroidal rotation velocity and pressure gradient of neon impurity measured with charge exchange spectroscopy [7] with a time resolution of 0.5 s at the mid plane in LHD (vertically elongated cross section) using radial force balance. The radial force balance equation can be expressed as

$$E_r = -\frac{1}{2n_I Z_I}\frac{\partial p_I}{\partial r} - (v_\theta B_\phi - v_\phi B_\theta) \qquad (1)$$

where $B_\phi$ and $B_\theta$ are the toroidal and poloidal magnetic fields and $Z_I$, $n_I$ and $p_I$ are the ion charge, density and pressure of the measured impurity, respectively.

## 2. Magnetic island produced by the $n/m = 1/1$ perturbation coil

LHD has $n/m = 1/1$ external perturbation coils. The size of the magnetic island can be controlled up to 10 cm by changing the current of the perturbation coils. The spatial resolution of the measurements of the radial electric field using charge exchange spectroscopy is determined by the length of integration of the signal along the line of sight within the beam width of the neutral beam. The spatial resolution becomes poor near the plasma centre and relatively good near the plasma edge, and it is $\pm 1.5$ cm at $R = 4.05$ m.

Figure 1($a$) shows the poloidal cross section of the last closed magnetic flux surface and magnetic island calculated (with zero beta) for the discharge with the $n/m = 1/1$ external perturbation coil current of $-1200$ A. Figures 1($b$) and 2 show the electron density measured with an FIR laser interferometer, temperature profiles measured with a YAG laser Thomson scattering system and ion temperature profiles measured with charge exchange spectroscopy for plasmas with and without a magnetic island. The magnetic island is located near the plasma edge at $\rho = 0.85$. As shown in figures 1($a$) and ($b$), flattening of the electron density and temperature are observed for the plasmas with an island ($I_{n/m=1/1} = -1200$ A, $\langle n_e \rangle = 2.1 \times 10^{19}$ m$^{-3}$) and without an island ($I_{n/m=1/1} = -390$ A, $\langle n_e \rangle = 2.2 \times 10^{19}$ m$^{-3}$) as a reference. The magnetic field, B, is 2.83 T with a vacuum magnetic axis at 3.5 m. The flattening width of the electron temperature is considered to represent the width of the magnetic island in the plasma, which would not be identical to the width of the vacuum magnetic island due to the healing effect [2]. Since the YAG thomson scattering system is able to probe electron temperature profile

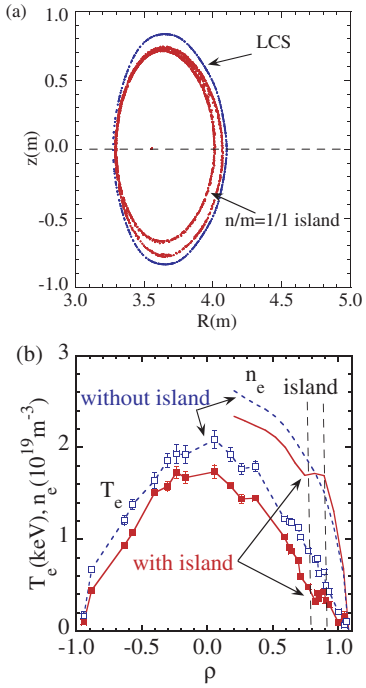


**Figure 1.** ($a$) Magnetic flux surface with 1/1 magnetic island and ($b$) radial profiles of electron density and temperature.

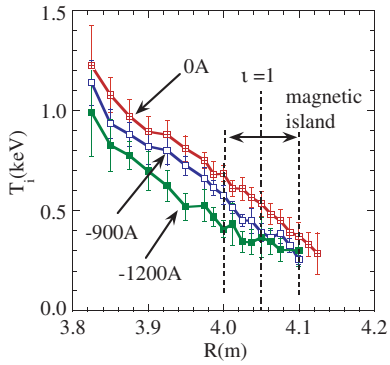


**Figure 2.** Ion temperature profiles with and without 1/1 magnetic island with a $n/m = 1/1$ perturbation coil current of 0, $-900$ and $-1200$ A.

in smaller plasma volumes and shorter time windows than ECE, it provide us a chance to investigate the fine structure of the electron temperature profile inside the magnetic island and may answer the question whether the electron temperature profile is completely flat or slightly peaked inside the magnetic island. However, at the moment, the accuracy of the YAG Thomson scattering measurements is not enough to give a conclusive answer to that question, and further improvement of the YAG Thomson system will be done in future.

The current of $n/m = 1/1$ external perturbation coils is varied in a wide range from 0 to $-1200$ A for the plasma with a magnetic field of 1.5 T, vacuum magnetic axis at 3.5 m and the averaged density of $\langle n_e \rangle = 1.2 \times 10^{19}$ m$^{-3}$. As the current of the $n/m = 1/1$ external perturbation coils is increased, the width of the island becomes larger as seen in figure 2. The flattening of ion temperature is observed in the plasma both without ($I_{n/m=1/1} = -900$ A) and with ($I_{n/m=1/1} = -1200$ A) a vortex-like plasma flow, discussed later. When the current

of the $n/m = 1/1$ external perturbation coils is small (see 0 A case in figure 3), no island structure appears in the profile of the radial electric field. As the perturbation coil current increases, the clear structure of the magnetic island appears in the radial electric field [8] and the width of the magnetic island estimated from the radial profiles of radial electric field increases up to 9 cm, which corresponds to 17% of the averaged minor radius. A large shear of the radial electric field is observed at the boundary of the magnetic island ($R = 4.00$ and 4.09 m).

Bifurcation of the plasma flow inside the magnetic island is observed. When the current of $n/m = 1/1$ external perturbation coils, $I_{n/m=1/1}$, becomes large enough (see $-1200$ A in figure 3), a finite radial electric field appears inside the magnetic island. The radial electric field is zero at the centre of the magnetic island, and the sign of the radial electric field is reversed across the centre of the island. Although a change in the sign of the plasma flow is observed in the O-point region of the large magnetic island, it is not observed in the X-point region of the magnetic island. There is no difference in the behaviour of the flow between the X-point region of the magnetic island and the plasma without a magnetic island. This observation indicates the existence of a vortex flow pattern inside the magnetic island. The plasma flow inside the magnetic island is due to the imbalance of the viscous force between the two boundaries at the O-point of the magnetic island. The plasma flow at the outward and inward boundaries at the O-point of the magnetic island are given as

$$V_{\text{outward}} = V_{\theta\text{X}} + \frac{W}{2}\frac{\partial V_{\theta\text{X}}}{\partial r} \tag{2}$$

$$V_{\text{inward}} = V_{\theta\text{X}} - \frac{W}{2}\frac{\partial V_{\theta\text{X}}}{\partial r} \tag{3}$$

where $V_{\theta\text{X}}$ and $(\partial V_{\theta\text{X}}/\partial r)$ are the poloidal flow velocity and the velocity shear at the X-point of the magnetic island with the width $W$, respectively. When the plasma rotates with velocity shear, there should be an energy source to sustain the velocity shear against the perpendicular viscosities. The power density, $P$, to sustain the plasma flow should be balanced against the energy dissipation due to the viscosities at the boundary and inside the magnetic island as

$$P = n_{\text{i}} m_{\text{i}} \left[ \mu_\delta \frac{(V - V_{\text{outward}})^2}{\delta} + \mu_\delta \frac{(-V - V_{\text{inward}})^2}{\delta} + \mu_W \frac{4V^2}{W} \right] \tag{4}$$

where $n_{\text{i}}$, $m_{\text{i}}$, $\mu_\delta$, $\mu_W$, $\delta$ and $V$ are the ion density, the ion mass, the viscosity at the boundary and inside the magnetic island, the shear width at the boundary of the magnetic island and the velocity of vortex-like flow inside the magnetic island, respectively. The velocity giving the minimum power, $P$, is considered to be the velocity of the vortex-like flow at the O-point, and it is given as

$$V_{\text{O}} = \frac{W^2}{4\delta}\frac{\mu_\delta}{\mu_W}\frac{\partial V_\theta}{\partial r} \tag{5}$$

The plasma flow velocity inside the magnetic island is proportional to the square of the island width when the viscosity at the boundary of the magnetic island, md, is constant. The direction of the flow (sign of $V_{\text{O}}$) is determined by the sign of the radial electric field shear $(\partial V_{\theta\text{X}}/\partial r)$ at the X-point of the magnetic island. The non-linearity of the anomalous viscosity [9] is required to cause the sudden appearance of plasma flow inside the magnetic island. It is expected that the anomalous viscosity, md, is small when there is no vortex-like flow and the velocity shear is localized at the boundaries, while it becomes large when the velocity shear region becomes wider associated with the appearance of vortex-like plasma flow inside the magnetic island. There is no observation that indicates hysteresis in the appearance of vortex-like plasma flow inside the magnetic island because the current of the perturbation coils is constant in time. The current ramp up and down experiment is necessary to investigate the hysteresis effect.

Flattening of the space potential is observed inside the magnetic island when the perturbation field is small as seen in figure 4. However the convective poloidal flow inside the island is observed when the magnetic island width exceeds a critical range (15–20%) of the minor radius. The vortex-like

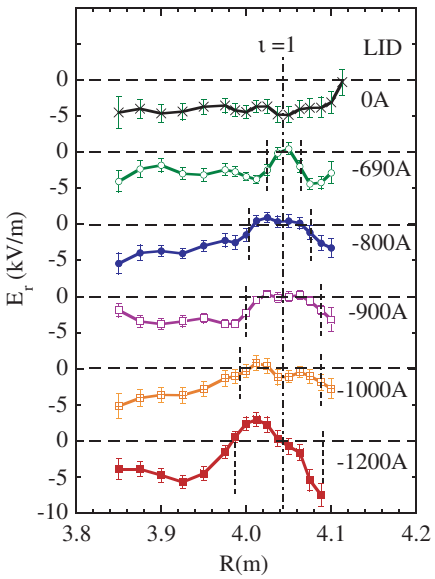


**Figure 3.** Radial profiles of radial electric field for various currents of $n/m = 1/1$ perturbation coil of 0, $-690$, $-800$, $-900$, $-1000$ and $-1200$ A.

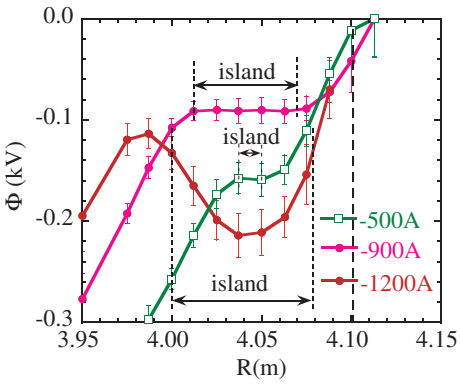


**Figure 4.** Radial profiles of space potential for various currents of $n/m = 1/1$ perturbation coil of $-500$, $-900$ and $-1200$ A. The typical error bar is 0.01–0.03 kV.

plasma flow results in a non-flat space potential ($\partial^2\Phi/\partial r^2 > 0$) inside the magnetic island. The sign of the curvature of the space potential is determined such as to decrease the shear of the poloidal flow at the boundary of the magnetic island.

These observations show that a bifurcation in flow pattern inside the magnetic island exists. When the size of the magnetic island is below the critical range, there is no plasma flow inside the magnetic island and velocity shear is localized at the boundary. The viscosity in the velocity region is expected to be reduced due to the velocity shear. However, the vortex-like plasma flow appears and the velocity shear region spreads inside the magnetic island when the size of the magnetic island exceeds the critical range. Here the viscosity in the velocity region is expected to increase due to a lack of localization of the velocity shear.

## 3. Cold pulse propagation inside the magnetic island

Since the radial profiles of the electron temperature show a flattening inside the magnetic island, transport analysis based on the temperature gradient and radial heat flux in the steady state is invalid. The localized flattening of the electron temperature profile is due to a modification of the magnetic topology resulting from the magnetic island produced by the perturbation field and not due to the increase in energy transport. When there is heating power inside the magnetic island, the temperature profile can have maxima inside the magnetic island, and the increase in electron temperature is determined by the balance between local heating power and thermal diffusivity. Since there is no Ohmic heating and the power deposition of the NBI is peaked at the plasma centre in LHD, the power density inside the magnetic island is negligible. This is in contrast to the experiment in the RTP tokamak [3], where the maxima of electron temperature are observed inside the magnetic island. A significant reduction in energy transport is expected inside the magnetic island because there is no pressure driven turbulence existing inside the magnetic island due to the flattening of the temperature and density profiles. In order to evaluate the transport inside the magnetic island, the response of the electron temperature to the cold pulse produced by a tracer-encapsulated solid pellet (TESPEL) [10] is investigated inside or at the boundary of the magnetic island [11].

When the $n/m = 1/1$ external perturbation coil current is negative, the O-point of the magnetic island is located at the outboard side and the X-point of the magnetic island is located at the inboard side. The cold pulse produced by TESPEL starts from the O-point of the magnetic island and propagates to the X-point of the magnetic island along the magnetic flux surface. Then the cold pulse propagating outside the magnetic island across the magnetic flux surface is measured with an ECE radiometer located at the inboard side. On the other hand, when the $n/m = 1/1$ external perturbation coil current is positive, the X-point of the magnetic island is located at the outboard side and the O-point of the magnetic island is located at the inboard side. Therefore, the $n/m = 1/1$ external perturbation coil current was set to be positive for the cold pulse experiment. This is in contrast to the experiment with negative current for the radial electric field measurements discussed before in which the O-point of the magnetic island should

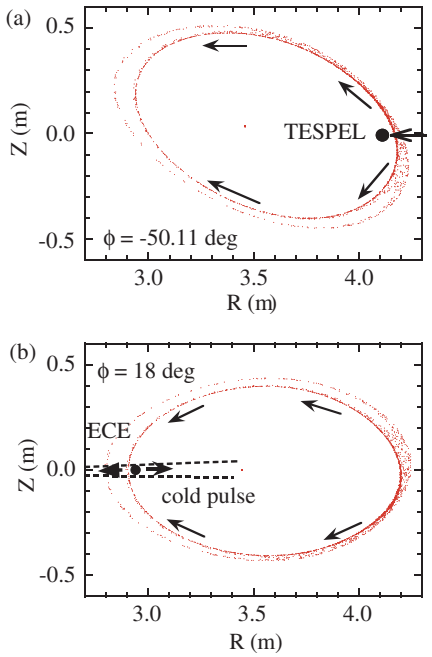


**Figure 5.** Magnetic flux surface with 1/1 magnetic island at (*a*) TESPEL injection and at (*b*) the ECE radiometer with a current of $n/m = 1/1$ perturbation coil of +800 A.

be located at the outboard side. Figure 5 shows the poloidal cross section of the magnetic flux surface at the toroidal angle $\phi = -50.1^\circ$, where the TESPEL is injected to produce a cold pulse, and at the toroidal angle $\phi = 18^\circ$, where the ECE radiometer is installed to measure the response of the cold pulse to the electron temperature. The ECE radiometer is located at the inboard side and TESPEL is injected from the outboard side of LHD 68° apart in the toroidal direction. The cold pulse produced at the X-point of the magnetic island propagates to the boundary of the magnetic island along the magnetic flux surface. Then the cold pulse propagates inside the magnetic island from the boundary across the magnetic flux surface.

Figure 6 shows the electron temperature profile measured with a ECE radiometer for the plasma with a magnetic axis at 3.5 m, a magnetic field of 2.88 T, and the averaged density of $\langle n_e \rangle = 1.7 \times 10^{19}\,\mathrm{m}^{-3}$. There is a clear flattening of the electron temperature observed at the O-point of the magnetic island. When the TESPEL is injected into the outboard X-point of the magnetic island, the cold pulse starts from the boundary of the magnetic island ($R = 2.95$ m) and propagates both inside ($R < 2.95$ m) and outside ($R > 2.985$ m) the magnetic island. The drop in the electron temperature due to the cold pulse is less than 10. The basic equation to determine the time evolution of electron temperature is given by

$$\frac{3}{2}n_e\frac{\partial}{\partial t}\delta T_e = -\nabla\cdot\left(\frac{\partial(-n_e\chi\nabla T_e)}{\partial\nabla T_e}\delta\nabla T_e + \frac{\partial(-n_e\chi\nabla T_e)}{\partial T_e}\delta T_e\right) \tag{6}$$

assuming the thermal diffusivity, $\chi$, is independent of electron temperature and its gradient is $\partial\chi/\partial T_e = 0$ and $\partial\chi/\partial\nabla T_e = 0$.

Then the diffusion equation can be simplified as

$$\frac{3}{2}n_e\frac{\partial}{\partial t}\delta T_e = \nabla\cdot n_e\chi\nabla\delta T_e \tag{7}$$

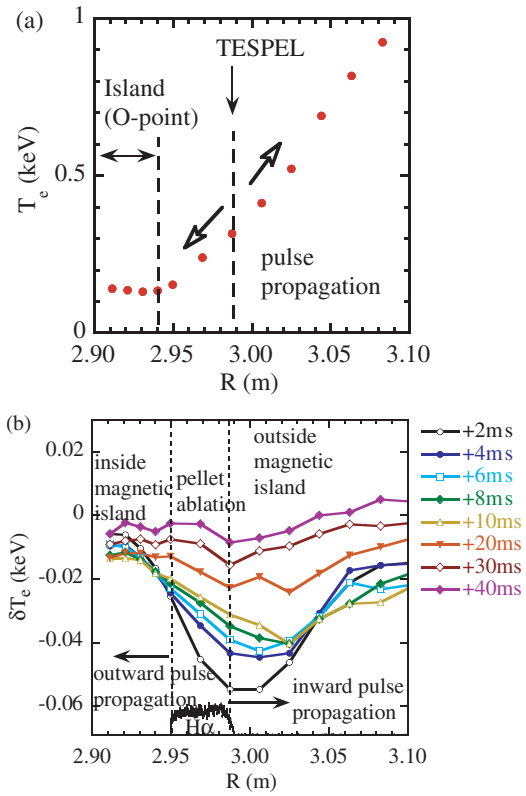


**Figure 6.** Radial profiles of (*a*) electron temperature, $T_e$, just before the TESPEL injection and (*b*) perturbation of electron temperature, d$T_e$, after the TESPEL injection at the O-point of the magnetic island. Here the arrows indicate the direction of propagation of the cold pulse.

The initial condition is chosen to match the time evolution of the electron temperature where the cold pulse starts ($R = 2.940$ m inside the magnetic island and $R = 2.987$ m outside the magnetic island). The thermal diffusivity and convective velocity are determined to match the time evolution of the electron temperature at a different chord ($R = 3.006$, 3.025, 3.044 m for outside the magnetic island and $R = 2.931$, 2.921, 2.911 m for inside the magnetic island). The time for propagation of the cold pulse indicated by the arrows is roughly proportional to $1/\chi$.

As shown in figure 7, the response time of the cold pulse inside the magnetic island is much longer than that observed outside the magnetic island. The amplitude of the cold pulse is also smaller inside the magnetic island than outside the island. The time delay and amplitude of the electron temperature of the cold pulse inside the magnetic island are reproduced by simulation of the cold pulse propagation in a slab model with a low thermal diffusivity of 0.3 m$^2$ s$^{-1}$, which is smaller than that (5 m$^2$ s$^{-1}$) outside the magnetic island by more than one order of magnitude. The sensitivity check of the simulation results to the given thermal diffusivity is investigated with the time evolution of the electron temperature 3–6 cm away from the start of the cold pulse as shown in figure 8. Since the sensitivity becomes weak as the thermal diffusivity increases, the uncertainty of the thermal diffusivity outside the magnetic island becomes large compared with that inside the magnetic island. The thermal diffusivity for the best fit to the experimental data is 0.3 m$^2$ s$^{-1}$ (with an uncertainty

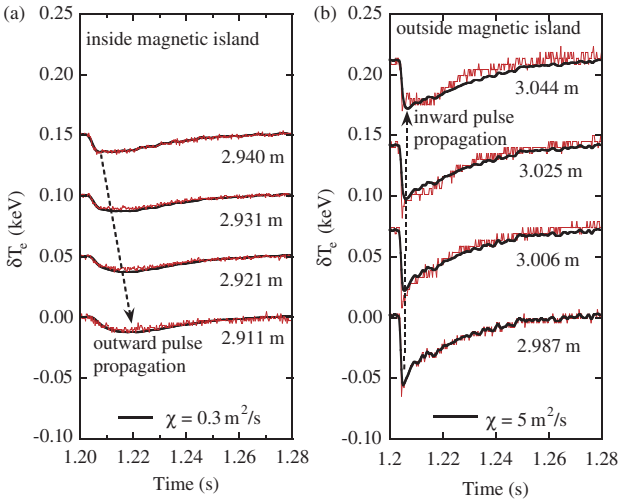


**Figure 7.** The time evolution of electron temperature measured with ECE (*a*) inside and (*b*) outside the magnetic island for the plasma where the TESPEL is injected. The thin lines represent the time evolution of the electron temperature measured with ECE, while the thick lines represent the simulated results using the slab model diffusion equations with the coefficient c. Here the arrows indicate the direction of propagation of the cold pulse.

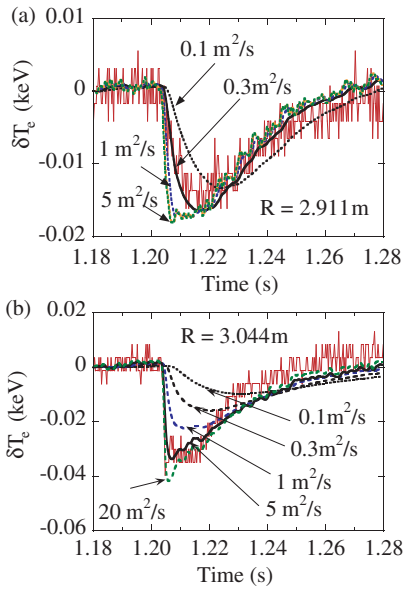


**Figure 8.** Comparison of measured electron temperature with that calculated with diffusion equations with different thermal diffusivity coefficients of 0.1, 0.3, 1, 5 and 20 m$^2$ s$^{-1}$ (*a*) inside (at $R = 2.911$ m) and (*b*) outside (at $R = 3.044$ m) the magnetic island.

factor of 2) inside the magnetic island and 5 m$^2$ s$^{-1}$ (with an uncertainty factor of 4) outside of the magnetic island.

The time evolution of the electron temperature after the pellet injection is well reproduced by the diffusive model in the slab model. This is because the increase in density due to the TESPEL is small enough not to enhance the turbulence and change the transport, which is in contrast to the experiment in Wendelstein VII-AS, where a large pellet triggers MHD oscillations [12]. However, the absolute value of the thermal diffusivity estimated here is uncertain due to the simplicity of the model used for the analysis because the structure of

the magnetic island (the effect of poloidal asymmetry) is not included in the analysis.

The structure of the radial electric field and heat transport at the magnetic island in LHD are investigated. The experimental results show the existence of a radial electric field shear at the boundary of the magnetic island for the plasma with the magnetic island size below the critical range. When the width of the magnetic island is large enough to exceed the critical range, a vortex-like flow inside the magnetic island appears due to the unbalance of viscosity between the two boundaries at the O-point of the magnetic island. The direction of the vortex-like flow is determined by the sign of the poloidal velocity shear at the X-point of the magnetic island. Although the existence of a critical range of the island size for the appearance of vortex flow implies non-linearity of viscosity at the magnetic island, a detailed comparison between the experiment and theoretical model is left to future work. The reduction in heat transport inside the magnetic island is experimentally confirmed by the cold pulse propagation experiment using TESPEL. Because of the poor spatial resolution, the thermal diffusivity inside the magnetic island is assumed to be constant in space.

Since there is a strong shear of the radial electric field, a further reduction of the thermal diffusivity is expected at the boundary of the magnetic island compared with inside the magnetic island. In this experiment, the thermal diffusivity inside the magnetic island is only measured for the plasma without vortex-like flow. An interesting topic is how the transport changes when the vortex-like flow appears. This issue will also be studied in the future. The combination of the radial electric field shear that appears at the boundary of the magnetic island and the significant reduction in thermal diffusivity inside the magnetic island would be one of the candidate mechanisms explaining the significant reduction in transport near the rational surface that is often observed in the internal transport barrier in tokamaks. The electron heat transport is improved at the boundary of the magnetic island as well as inside the magnetic island, and the magnetic island serves as a poloidally asymmetric transport barrier.

## Acknowledgments

The authors would like to thank the LHD technical staff for their effort to support the experiments in LHD. This work is partly supported by a grant-in-aid for scientific research of MEXT Japan.

## References

[1] Lopes Cardozo N.J. *et al* 1994 *Phys. Rev. Lett.* **73** 256
[2] Narihara K. *et al* 2001 *Phys. Rev. Lett.* **87** 135002
[3] Salzedas F. *et al* 2002 *Phys. Rev. Lett.* **88** 075002
[4] Yang X. *et al* 1991 *Phys. Fluids* B **3** 3448
[5] Hidalgo C. *et al* 2000 *Plasma Phys. Control. Fusion* **42** A153
[6] Fujiwara M. *et al* 2000 *Nucl. Fusion* **40** 1157
[7] Ida K., Kado S. and Liang Y. 2000 *Rev. Sci. Instrum.* **71** 2360
[8] Ida K. *et al* 2002 *Phys. Rev. Lett.* **88** 015002
[9] Shaing K.C. 2002 *Phys. Plasmas* **9** 3470
[10] Sudo S. *et al* 2002 *Plasma Phys. Control. Fusion* **44** 129
[11] Inagaki S. *et al* 2004 Observation of reduction of heat transport inside the magnetic island in the large helical device *Phys. Rev. Lett.* at press
[12] Lyon J. 1997 *Proc. 24th EPS Conf. (Berchtesgaden)* vol 21A, p 1629